Proceedings of the Institute of Acoustics

SPATIAL STRUCTURE OF SOUND IN THE OCEAN - TRANSFER FUNCTIONS AND SOUND STREAMERS

B.J. Uscinski(1), M J Stirland(2)

(1) Department of Applied Mathematics and Theoretical Physics, University of Cambridge, Cambridge, CB3 9EW
(2) Marconi Maritime Applied Research, Cambridge, CB4 4FX

1. INTRODUCTION

Two experiments were performed in 1985 and 1986 in the Mediterranean to study the spatial structure of sound propagating through random irregularities in the ocean. In the first trial broadband acoustic signals were recorded close to the source, and then by a 65m vertical array at a distance of 5 km. The Ocean Transfer Function (OTF) was obtained by deconvolving the signals by means of an algorithm that uses powerful physical constraints arising from scattering theory. The OTF was calculated in both time and frequency (250-2000Hz) domains for the five days of the trial, allowing study of the vertical spatial structure of sound propagating in inhomogeneities whose longitudinal scale is larger than the acoustic path.

In the second trial the longitudinal and vertical structure of the sound field was investigated over ranges of 4 km and depths of 400 m. Streamers of enhanced acoustic intensity were observed whose length and thickness agreed well with predictions of both theory and numerical simulations.

2. OCEAN TRANSFER FUNCTION

The first experiment was carried out in the Tyrrhenian Sea. The source, a small explosive charge, was situated at a depth of 400 m with a reference array nearby to record the emitted signature. The signals received at a distance of 5 km by a 65 m vertical array with top at a depth of 224 m were relayed by radio to the research vessel Maria Paolina G. A total of 229 events were recorded during the five days of the trial, while at the same time continuous sound speed measurements were made with a Towed Oscillating Body between 25 and 250 m, together with 4 deeper CTD and 70 XBT casts. The resulting sound speed profile is shown in Fig. 1 together with the principal eigen-rays. These include a direct path, a sub-surface refracted and surface reflected paths.

The sound speed also contained weak randomly irregular features whose spatial autocorrelation function $R(g)$ could be described by

$$R(g) = \exp(-g)(1 - g/\ell_2 + g^2/\ell_3^2) \qquad (1)$$

where

$$g^2 = \xi^2/L_H^2 + \varsigma^2/L_V^2 \quad . \qquad (2)$$

Here ξ and ς are separations in the horizontal and vertical directions, and L_H and L_V are the corresponding scale sizes. In the vicinity of the direct ray

$$L_V = 68\ m,\ L_H = 6\ km,\ \ell_2 = 0.45 \text{ and } \ell_3 = 1.60 \quad .$$

The variance of the random component was estimated to be

5×10^{-9} of the mean sound speed between 220 and 270 m,
1.5×10^{-9} between 270 and 330 m, and 1×10^{-9} below this.

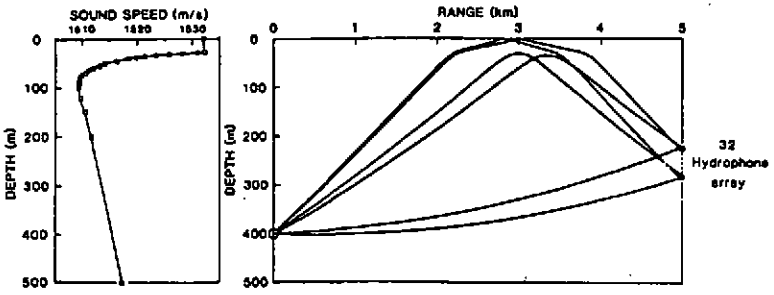

Fig. 1: Mean sound speed profile and principal eigen-rays for the NAPOLI 85 trial

An important feature is the layer with an enhanced sound speed variance at about 300 m, due, it is believed, to the presence of intrusions of Levantine intermediate water (LIW). Analysis also showed that only about 25% of the sound speed inhomogeneities could be due to internal waves, and that the main effect was due to the mixing intrusions of LIW.

A typical signature $S(t)$, recorded close to the source, is shown in Fig. 2 together with the response $R(t)$ at the far array. The contributions due to the three paths are clear. The effect of the ocean medium in converting $S(t)$ into $R(t)$ is called the Ocean Transfer Function (OTF), $T(t)$

$$R(t) = \int S(t')T(t-t')dt' \quad . \tag{3}$$

Determining $T(t)$ from (3) is a difficult task since, in general, experimental data do not contain sufficient information to allow a unique solution to be obtained. For this reason it is often necessary to supplement the experimental $R(t)$ and $S(t)$ with additional constraints based on a knowledge of the physics of the situation. In this case a minimization procedure related to the method of least squares was used with two constraints. The first constraint required that the OTF be non-negative, while the second set limits on the mean width of the OTF. These constraints derive from the properties of wave propagation in random media, and on the measured characteristics of the irregular component of the sound speed described above.

A typical OTF is shown in Fig. 3. The most important features of the OTF are the existence of two peaks, and the narrow widths of these peaks. These characteristics are common to almost all the OTF's.

SPATIAL STRUCTURE OF SOUND IN THE OCEAN

Fig. 2: From left to right, $S(t)$ and $R(t)$ (direct path, surface reflected and sub-surface refracted paths)

These main features of the OTF can be assigned explanations consistent with the structures observed in the sound-speed field. The second arrival in the OTF is believed to

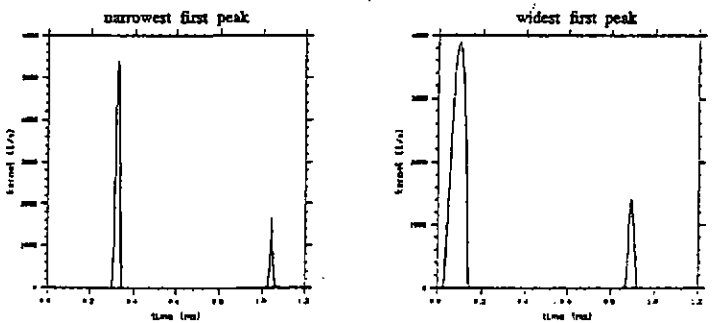

Fig. 3: Typical OTF's for the direct path showing the main and second arrivals separated by about 0.8 m sec. The widths of the main peaks vary between 0.04 - 0.12 m sec.

be due to the layer-like feature at about 300 m depth. This seems to be a quasi-deterministic structure that retains its general shape throughout the five days of the trial but whose vertical position varies slowly. This could result in the splitting of the direct ray to produce a second path. Preliminary estimates indicate that the observed time lag is consistent with the size and refractive index variation of the layer, and the expected geometry of such a second path.

The narrow width of the peaks in the OTF indicates that they have a very wide frequency spectrum, much wider in fact than the bandwidth of the observed signals $S(t)$, $R(t)$, which have upper frequency limits of about 2 kHz. This is one of the main difficulties in carrying out the deconvolution (3), and also means that it is not possible to obtain any detailed structure in the OTF. The most that can be reliably concluded in this regard is that peaks in the OTF vary in width by a factor of about three during the course of the trial.

SPATIAL STRUCTURE OF SOUND IN THE OCEAN

3. TIME-SPACE STRUCTURE OF INTENSITY FLUCTUATIONS

By selecting the main peak of the OTF and representing it in the frequency domain it was possible to determine the intensity of the received signal at each hydrophone for a particular frequency band. We now concentrate on the first peak in the ocean transfer functions thus restricting our selves to considering just one macropath between the source and the receiver.

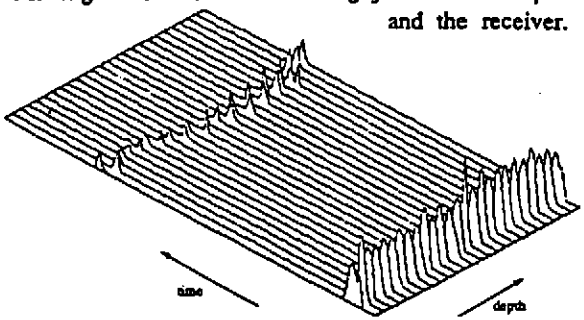

Fig. 4: Main and second arrivals down the vertical array. The maxima of the main arrivals have been aligned to show the variation in arrival time of the second spike.

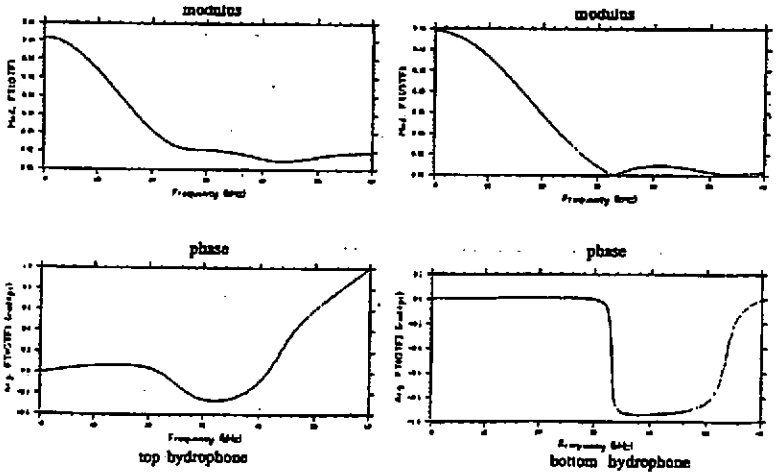

Fig. 5: The modulus and phase of the Fourier transforms of the first peak in the ocean transfer function for the top and bottom hydrophones in the receiving array for the same event as that shown in Fig. 4 For the purpose of these calculations the time origin is taken to be at the maximum value of the ocean transfer function

SPATIAL STRUCTURE OF SOUND IN THE OCEAN

4. SOUND STREAMERS

The Ocean Transfer Functions obtained in the NAPOLI 85 trial exhibit strength variations down the vertical array with a scale of about 15 m. This spatial structure in the acoustic signal is part of a more complex picture that was first revealed in numerical simulations of sound propagation in a medium with spatial random variations of acoustic refactive index.

The spatial pattern of intensity fluctuations produced when a 3.5 kHz acoustic wave propagates through an ocean internal wave field at a depth of 100 m is shown in Fig. 6 on the left as given by numerical simulation. Only part of the ocean volume is shown. The dimensions are given and we note that the most striking features are the strong spikes of intensity that arise and extend over large distances in the direction of sound propagation. Enclosing these high intensity regions by contours produces a new picture, that of patches where the sound has been concentrated. A contour picture of this type corresponding to the simulation is given on the right of Fig. 6 with the dimension transverse to the direction of sound propagation added. Since the internal wave irregularities have horizontal and vertical scales that are in the ratio of about ten to one, so also the intensity fluctuations exhibit a similar anisotropy. However, the logitudinal scale of the sound patches in the direction of propagation is even greater.

Simple analysis shows that in the region of well developed intensity fluctuations the vertical, transverse, and longitudinal scales of high intensity sound patches are respectively

$$\varsigma_0 = L_V/\sqrt{2\Gamma X}, \eta_0 = L_H/\sqrt{2\Gamma X}, \xi_0 = kL_V^2/2X \qquad (4)$$

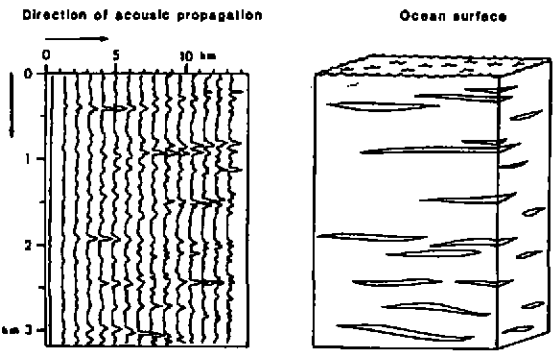

Fig. 6: Simulated acoustic intensity fluctuations and a contour diagram of the high intensity ribbons

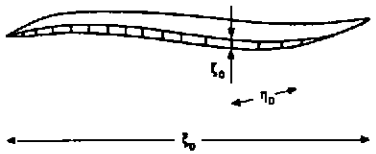

Fig. 7: Typical ribbon of high acoustic intensity

where L_V and L_H are the vertical and horizontal scales of the internal wave irregularities,

$$X = x/kL_V^2 \quad , \tag{5}$$

x being the distance in the direction of propagation, and Γ is a parameter characterizing the strength of the scattering regime involved. In the 3.5 kHz case illustrated in Fig. 6 the quantities turn out to be, when the range x is about 10 km,

$$\zeta_0 = 20\ m,\ \eta_0 = 317\ m,\ \xi_0 = 5.8\ km \quad . \tag{6}$$

The high intensity patches appear as flat ribbons of concentrated sound, greatly extended in the direction of propagation. They tend to lie at small angles above and below the horizontal and to be separated one from the other by some characteristic distance in the vertical. A typical ribbon is shown in Fig. 7 for the 3.5 kHz example under discussion.

5. EXPERIMENTAL OBSERVATION OF THE HIGH INTENSITY STREAMERS

In 1986 an experiment was carried out in the eastern Mediterranean to map out the predicted intensity streamers in the ocean. A moored acoustic source transmitted pulses with a 3.5 kHz carrier frequency over distance of some 10 km. The resulting irregular acoustic field was recorded by a 64 m vertical array deployed from the Maria Paolina G

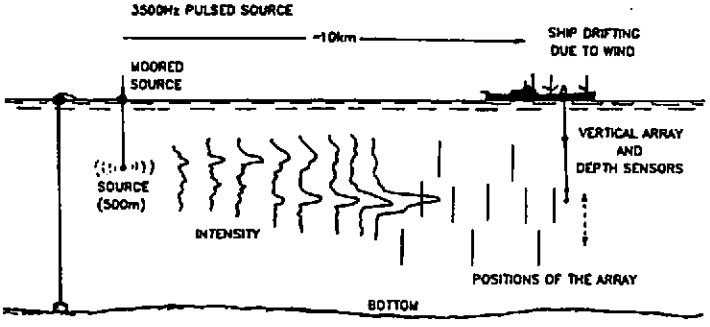

Fig. 8: Experiment to map the sound ribbons. The source transmits pulses at a carrier frequency of 3.5 kHz.

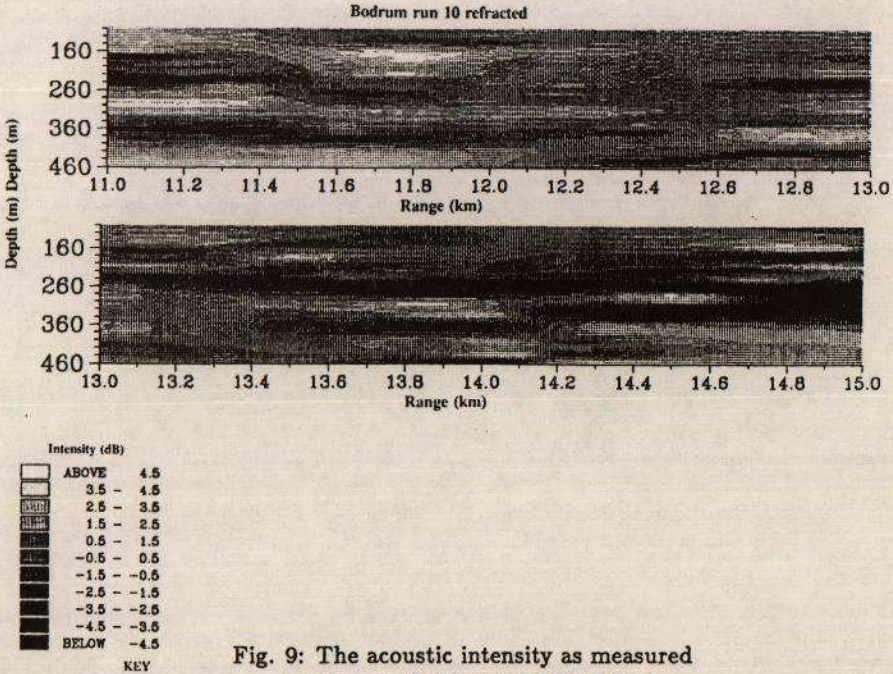

Fig. 9: The acoustic intensity as measured experimentally for a 3.5 kHz pulsed source. The long high intensity ribbons can be clearly seen.

(Fig. 8). The intensity, averaged over ten pulses, was recorded as a function of distance down the array. The array was then lowered by a distance equal to its own length and the process was repeated until a depth of several hundred meters had been covered. The array was then raised and the procedure continued in the same manner. At the same time the ship drifted with wind and current at a constant rate of about 3 km/h so that the acoustic intensity structure could be mapped in a strip several hundred meters deep and several kilometers long. Fig. 9 shows an intensity plot resulting from one of the drifting sequences described above. The predicted scales of 20 m in the vertical and over five kilometers in the direction of propagation are seen to be close to the characteristics of the measured ribbons. Finally, Fig. 10 shows the same intensity ribbons presented in a different manner, plotted like hills and valleys in perspective from above and with the lognitudinal scale much compressed.

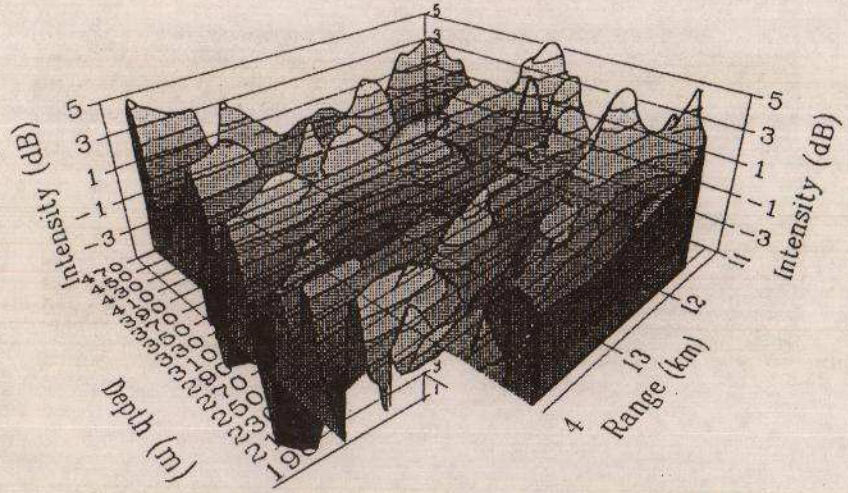

Fig. 10: The acoustic intensity ribbons of Fig. 9 presented as a contour plot in perspective. The scale in the direction of propagation is now much compressed.

6. ACKNOWLEDGEMENTS

The two experiments described above were undertaken as a cooperative venture by the SACLANT Undersea Research Centre, La Spezia, Italy and the Ocean Acoustics Group, DAMTP, University of Cambridge, U.K. Dr B J Uscinski was supported by the U.K. Ministry of Defence, Procurement Executive. Figs. 9 and 10 are reproduced with kind permission from the Acoustics Bulletin. Processing of the acoustic data to obtain the Ocean Transfer Functions was carried out by Marconi Maritime Applied Research, Cambridge.

7. REFERENCES

[1] B J USCINSKI, J R POTTER & T AKAL, 'Broadband Acoustic Transmission Fluctuations During NAPOLI 85', an experiment in the Tyrrhenian Sea: Preliminary results and an arrival-time analysis, J. Acoust. Soc. Am. Vol. 86, pp 706-715.

[2] L Ju FRADKIN, Identification of the Acoustic Ocean Transfer Function in the Tyrrehen Sea, I: Statistical Considerations, I: Physical Considerations, J. Acoust. Soc. Am. (in press)

[3] B J USCINSKI & J R POTTER, Sound Ribbons in the Sea, Acoustics Bulletin, 1988, Vol. 13, pp 24-28